Thermochimica Acta 509 (2010) 100–110

Contents lists available at ScienceDirect

Thermochimica Acta

journal homepage: www.elsevier.com/locate/tca

Carbochlorination of yttrium oxide

J.P. Gaviría [a,b,*], A.E. Bohé [a,b,c]

[a] División Cinética Química - Complejo Tecnológico Pilcaniyeu, Centro Atómico Bariloche - Comisión Nacional de Energía Atómica, Av. Bustillo km 9500 (8400), S.C. de Bariloche, Río Negro, Argentina
[b] Consejo Nacional de Investigaciones Científicas y Técnicas, Argentina
[c] Centro Regional Universitario Bariloche, Universidad Nacional del Comahue, Argentina

ARTICLE INFO

Article history:
Received 31 March 2010
Received in revised form 4 June 2010
Accepted 9 June 2010
Available online 16 June 2010

Keywords:
Yttrium oxide
Carbochlorination
Yttrium oxychloride
Carbon–chlorine interaction
YCl_3 evaporation

ABSTRACT

The reaction of chlorination of a mixture composed by Y_2O_3 and sucrose carbon was studied by thermogravimetry over a temperature range of 550–950 °C. The reaction proceeds through several successive stages. The first of them is the formation of solid yttrium oxychloride (YOCl) and subsequently the YOCl is carbochlorinated to produce YCl_3 (solid or liquid, depending on the temperature) in two stages. The stoichiometries of the first stage and the global reaction were estimated by mass balances, taking into account the chlorine adsorbed by the remainder carbon. The results showed that the reactions involved progress with the formation of CO_2 and CO in the temperature range of 600–775 °C. The interaction between sucrose carbon and chlorine was analyzed by thermogravimetry in order to quantify the amount of chlorine which is adsorbed on its surface. It was studied the effect of the temperature and initial mass of carbon. The morphological analysis performed by SEM of partially reacted samples showed that the formation of YOCl proceeds through a mechanism of nucleation and growth. For temperatures above 715 °C the final product of the carbochlorination is liquid YCl_3, whose evaporation is observed in the thermogravimetry. The evaporation kinetics was analyzed in argon atmosphere and from the thermogravimetric curves was determined a value of 250 kJ/mol for the heat of evaporation of YCl_3. This value is consistent with a partial dimerization of the gaseous chloride.

1. Introduction

The carbochlorination of metallic oxides is a very important process in the industrial production of pure metals. There are many metallic oxides that can be transformed to metals through a process which consist of three stages [1–3]. In the first, the carbochlorination stage, the oxide reacts with chlorine in presence the carbon to produce the metallic chloride. Subsequently, the metal is obtained from the reduction of the chloride. Finally, the metallic sponge is purified by high temperature vacuum distillation.

Reductant species like carbon or carbon monoxide decrease the potential of oxygen, favoring the formation of the chloride. Carbon has catalytic activity sites where it is possible the formation of highly reactive gas intermediates, such as monoatomic chlorine ($Cl^{\bullet}$) [4,5], phosgene ($COCl_2$) [6] or oxychlorides [7]. Most of the authors propose that the carbochlorination reaction happens through gas intermediates. Bergholm [8] and Barin and Schuler [4] demonstrated that the direct contact between oxide and carbon particles is not necessary for the progress of the reaction. Several authors propose that $Cl^{\bullet}$ is the most probable intermediate; Barin found that the kinetic effect of the carbon in the carbochlorination of TiO_2 disappears when the distance between the particles of oxide and carbon is higher than the mean free path of $Cl^{\bullet}$. Amorebieta and Colussi [9] and Pasquevich [10] studied the interaction between $Cl_2(g)$ and sucrose carbon by mass spectroscopy and verified the presence of $Cl^{\bullet}$ in the gas phase at temperatures below 1000 °C. Pasquevich detected them at 900 °C, an approximate temperature since the chlorine atoms can be recombined on the glass walls, which conducted the reactor gases to the spectrometer. Amorebieta utilized passive glass and found $Cl^{\bullet}$ from 677 °C.

There are in literature only a few works concerning to the chlorination or carbochlorination of yttrium oxide or minerals containing this rare earth. Miller et al. [11] presented a method to synthesize anhydrous rare earth chlorides, included YCl_3. The method is based on the reaction between oxides or mixture of oxides with gaseous carbon tetrachloride (CCl_4) in a temperature range of 500–650 °C. In a previous work [12] we analyzed the kinetics of the chlorination of yttrium oxide. The results showed that yttrium oxychloride is formed in an initial stage. For temperatures above 800 °C, the YOCl is chlorinated leading to the production of liquid YCl_3. The chloride has a considerable vapor pressure, and the evaporation rate

* Corresponding author at: División Cinética Química - Complejo Tecnológico Pilcaniyeu, Centro Atómico Bariloche - Comisión Nacional de Energía Atómica, Av. Bustillo km 9500 (8400), S.C. de Bariloche, Río Negro, Argentina.
Tel.: +54 02944 445293; fax: +54 02944 445293.
E-mail address: gaviriaj@cab.cnea.gov.ar (J.P. Gaviría).

0040-6031/$ – see front matter © 2010 Elsevier B.V. All rights reserved.
doi:10.1016/j.tca.2010.06.009

is higher than its production rate. Braginski et al. [13], Gimenes and Oliveira [14] and Augusto and Oliveira [15] studied the carbochlorination of the yttrium oxide and xenotime (mineral rich in heavy rare earths, [16]). They found that the YOCl is an intermediate product previous to the formation of the YCl_3.

The reactions proposed by these authors are the followings:

Braginski (1100 °C):

$$Y_2O_3(s) + C(s) + Cl_2(g) \rightarrow 2YOCl(s) + CO(g) \quad (1)$$

$$YOCl(s) + C(s) + Cl_2(g) \rightarrow YCl_3(l) + CO(g) \quad (2)$$

Gimenes (600–950 °C):

$$2YPO_4(s) + C(s) + 2Cl_2(g) \rightarrow 2YOCl(s) + P_2O_5(s) + COCl_2(g) \quad (3)$$

$$2YOCl(s) + C(s) + 2Cl_2(g) \rightarrow 2YCl_3(s, l) + CO_2(g) \quad (4)$$

Augusto (600–900 °C):

$$YPO_4(s) + 1/2CCl_4(g) \rightarrow YOCl(s) + 1/2P_2O_5(s) + 1/2COCl_2(g) \quad (5)$$

$$YOCl(s) + 1/2CCl_4(g) \rightarrow YCl_3(s, l) + 1/2CO_2(g) \quad (6)$$

The objective of this work is to elucidate the reaction stages of the carbochlorination of Y_2O_3, to analyze the influence of the temperature on these stages and to propose their stoichiometry. The final product of the reaction is liquid YCl_3, which has a considerable vapor pressure at the temperatures studied. The kinetics of its evaporation was analyzed and the evaporation heat was obtained.

2. Experimental

2.1. Materials

Solid reactants used were an yttrium oxide powder 99.99 pct (Aldrich Chemical Company, Inc., Milwaukee, MI) and sucrose carbon. The mean particle size of the oxide measured by laser diffraction was 10 μm and showed a size distribution highly homogeneous (Mastersizer, Malvern Instruments Limited, Worcestershire, UK). Carbon was obtained from the pyrolysis of sucrose (Fluka Chemie AG) in inert atmosphere at 980 °C during 48 h and sieved to a size of 400 mesh (ASTM, square aperture of 37 μm). Carbon characteristics are well described by Gonzalez et al. [17]. Amorebieta and Colussi [9] and Pasquevich [10] utilized sucrose carbon and determined by mass spectroscopy that this type of carbon does not have volatile organic residues at the reaction conditions. The oxide and carbon powder have a BET surface area of 3.7 and 7.2 m^2/g, respectively (Digisorb 2600 Micrometeritics Instrument, Norcross, GA). Respective amounts of the solid reactants were weighed and mixed mechanically to obtain mixtures of Y_2O_3–C in the range of 6.7–16.7 pct (w/w, carbon mass/total mass).

Gases used were Cl_2 99.8 pct purity (Indupa, Bahía Blanca, Argentina) and Ar 99.99 pct purity (AGA, Buenos Aires, Argentina).

Solids were analyzed by X-ray diffraction (XRD) (Philips PW 1310-01), scanning electron microscopy (SEM) and energy dispersive spectroscopy (EDS) (SEM 515, Philips Electronic Instruments).

2.2. Thermogravimetric system

The measurements were performed using a thermogravimetric analyzer (TGA), which has been described elsewhere [18]. It consists of an electrobalance (Cahn 2000, Cahn Instruments, Inc., Cerritos, CA) adapted to work with corrosive atmospheres, a vertical tube furnace, a gas line, and a data acquisition system. The sensitivity of the system is ±5 μg while operating at 1000 °C under a gas flow rate of 9 L/h, measured at normal temperature and pressure. Each sample was placed in a cylindrical quartz crucible (7.8-mm inner diameter, 3.3-mm deep), which hangs from one of the arms of the electrobalance through a quartz wire. A quartz hangdown tube (4.6-cm diameter) carried the gases to the sample. The temperature of the sample was measured using a Pt–Pt (10 pct Rh) thermocouple encapsulated in quartz, which was placed 2 mm below the crucible. Flows of Ar and Cl_2 were controlled by means of flow meters and they were dried by passing through silica gel and $CaCl_2$, respectively. The mass changes were acquired every 2.5 s.

2.3. Procedure

Non-isothermal and isothermal measurements were made. In the non-isothermal runs the samples were kept 1 h under flowing Ar to purge the gas line and heated at 100 °C to eliminate water. Then the chlorine gas was introduced to the reaction zone and the samples were heated in the Ar–Cl_2 mixture up to 950 °C. The linear heating rate used was 3.8 °C/min. Mass changes and temperature were continuously monitored during the heating and the apparent mass change was taken into account to correct the experimental data [18]. In the isothermal runs the samples were heated in flowing Ar until the reaction temperature was reached. Once the temperature was stabilized, chlorine was admitted into the hangdown tube while mass changes were continuously monitored. The data were carefully analyzed to determine the reaction zero time.

3. Results and discussion

3.1. Thermodynamic considerations

The following reactions are possible in the Y_2O_3–C–Cl_2 system:

$$Y_2O_3(s) + Cl_2(g) \rightarrow 2YOCl(s) + 1/2O_2(g) \quad (7)$$

$$Y_2O_3(s) + 1/2C(s) + Cl_2(g) \rightarrow 2YOCl(s) + 1/2CO_2(g) \quad (8)$$

$$Y_2O_3(s) + C(s) + Cl_2(g) \rightarrow 2YOCl(s) + CO(g) \quad (9)$$

$$1/3Y_2O_3(s) + Cl_2(g) \rightarrow 2/3YCl_3(s, l) + 1/2O_2(g) \quad (10)$$

$$1/3Y_2O_3(s) + 1/2C(s) + Cl_2(g) \rightarrow 2/3YCl_3(s, l) + 1/2CO_2(g) \quad (11)$$

$$1/3Y_2O_3(s) + C(s) + Cl_2(g) \rightarrow 2/3YCl_3(s, l) + CO(g) \quad (12)$$

The production of $COCl_2(g)$ was not proposed due to two reasons: (1) it was not detected in the carbochlorination reactions with sucrose carbon [10], (2) $COCl_2$ decomposes forming CO and Cl_2 at temperatures above 650 °C [19].

The reduction of the oxide by carbon is not considered since it has a very highly value of ΔG^0 at the range of temperature used in this work (1082 and 865 kJ/mol for 600 and 1000 °C, respectively [20]). Nevertheless, the interaction between Y_2O_3 and sucrose carbon in argon atmosphere was analyzed by thermogravimetry at 950 °C and no mass change was observed. The XRD analysis of the sample after the treatment showed only the diffraction lines of Y_2O_3.

Fig. 1 shows the standard Gibbs free energy for the above reactions mentioned except reaction (10) which is the only one that has a positive value of ΔG^0. The calculations were performed with the HSC 6.12 Software [20] and the reactions were taken per mole of chlorine. The YOCl thermodynamic data used were extrapolated from values reported by Patrikeev et al. [21].

The reactions can be compared, assuming that the reactive systems involved are independent from each other. The curves show that the carbochlorination of Y_2O_3 to produce YOCl (reactions (8) and (9)) are more feasible to occur than: (1) direct chlorination

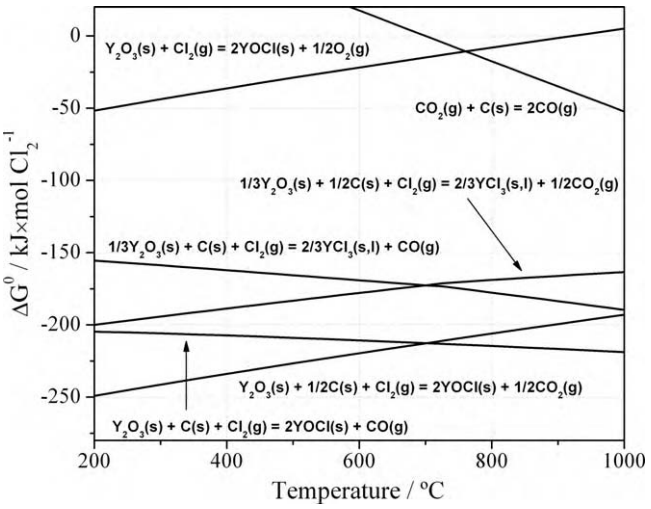

Fig. 1. Standard Gibbs free energy (per mole of chlorine) vs. temperature for reactions involved in the Y_2O_3–C–Cl_2(g) system.

to produce YOCl (reaction (7)), (2) carbochlorination of the oxide to produce YCl_3 (reactions (11) and (12)). On the other hand, the reactions which produce CO_2(g) have lower values of ΔG^0 for temperatures below to 701 °C, while at higher temperatures the formation of CO(g) is more convenient. This behaviour is due to the Boudouard reaction:

$$CO_2(g) + C(s) \rightarrow 2CO(g) \quad (13)$$

which has negative values of ΔG^0 for temperatures above 701 °C [20].

Fig. 2 shows the phase stability diagram of Y–O–Cl system at 600 and 1000 °C (data obtained from [20]). The axes are the partial pressure of O_2 and Cl_2, and the experimental conditions of them are indicated. This diagram shows that there is not a thermodynamic equilibrium between Y_2O_3 and YCl_3; therefore YOCl has to be formed previous to the formation of YCl_3 from Y_2O_3.

The results of the thermodynamic calculations indicate that YOCl is produced in a first stage of the reaction. Then, the YOCl can react through the following reactions:

$$YOCl(s) + Cl_2(g) \rightarrow YCl_3(s,l) + 1/2O_2(g) \quad (14)$$

$$YOCl(s) + 1/2C(s) + Cl_2(g) \rightarrow YCl_3(s,l) + 1/2CO_2(g) \quad (15)$$

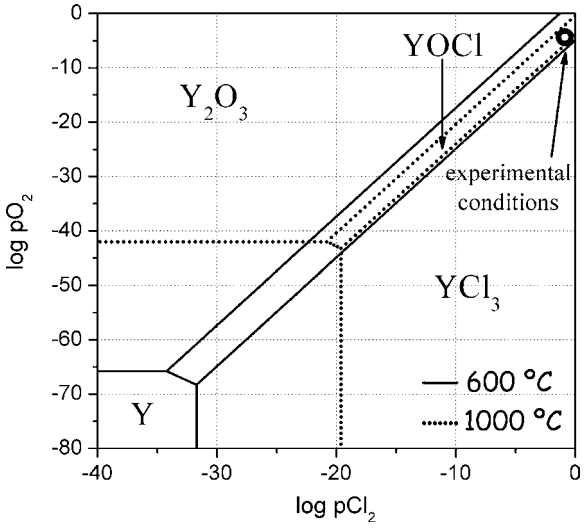

Fig. 2. Phase stability diagram of Y–O–Cl system at 600 and 1000 °C. The experimental conditions are indicated.

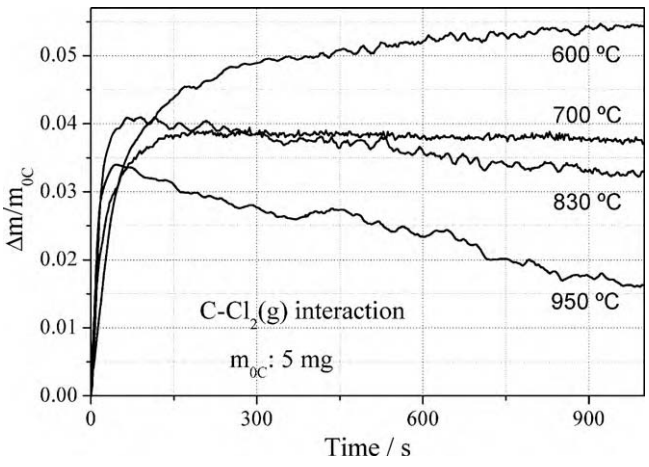

Fig. 3. Relative mass change vs. time in the C–Cl_2(g) interaction.

$$YOCl(s) + C(s) + Cl_2(g) \rightarrow YCl_3(s,l) + CO(g) \quad (16)$$

$$YOCl(s) \rightarrow 1/3Y_2O_3(s) + 1/3YCl_3(s,l) \quad (17)$$

$$YOCl(s) + 1/4O_2(g) \rightarrow 1/2Y_2O_3(s) + 1/2Cl_2(g) \quad (18)$$

Reactions (14) and (17) have positive values of ΔG^0 in all range of temperature analyzed, whereas reaction (18) (which is the reverse reaction of reaction (7)) has positive values of ΔG^0 for temperatures below 921 °C (see Fig. 1). Reactions (15) and (16) have negative ΔG^0 values, therefore the formation of YCl_3(s,l) will progress preferably through carbochlorination of YOCl.

3.2. Interaction C–Cl_2

The interactions produced between chlorine and carbon surface are solid–gas processes and can be classified inside of physical and chemical phenomena [22]. They involve physical and chemical adsorption, reaction between chlorine atoms with surface hydrogen atoms and micropore diffusion [17,23,24]. Landsberg et al. [25] investigated the carbochlorination of zirconium dioxide and found that the interaction does not originate C_xCl_y compounds.

In the present study, this interaction was analyzed by thermogravimetry and the effect of the temperature and initial mass were evaluated. The main objective was to obtain the mass change in the carbochlorination of Y_2O_3 that corresponds to the interaction between C and Cl_2. The experimental conditions used were a partial pressure of chlorine (pCl_2) of 35 kPa and an Ar–Cl_2 total flow (Q_{Ar-Cl_2}) of 4 L/h.

Fig. 3 shows the time evolution of the relative mass change ($\Delta m/m_{0C}$, where m_{0C} is the carbon initial mass) for the interaction C–Cl_2 at temperatures between 600 and 950 °C. The carbon initial mass used was 5 mg. The curves show that *maximum relative mass gain* (*qm*) diminishes with increasing temperature, taking a value of 0.054 and 0.034 for 600 and 950 °C, respectively.

The effect of the initial mass at 600 and 830 °C is shown in Fig. 4. These curves show that there is not a definite tendency of *qm* with the *initial mass of carbon*, since the value of *qm* reached using 15 mg is in the middle of the values obtained for 3 and 5 mg. These results are showing that the initial mass does not influence on the *qm* value and an initial mass of 5 mg was selected to determine the temperature dependence of *qm* (Fig. 5). These curves will be used in the system Y_2O_3–C–Cl_2 to estimate the mass gain due to the C–Cl_2 interaction.

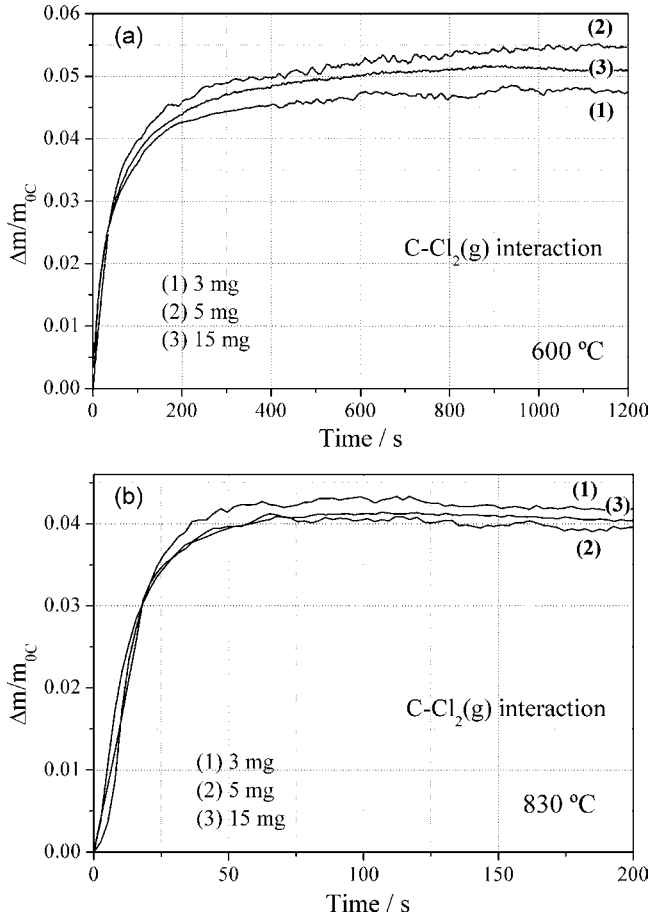

Fig. 4. Effect of the initial mass of carbon on the C–Cl_2(g) interaction. (a) 600 °C and (b) 830 °C.

3.3. Non-isothermal thermogravimetries

Fig. 6 shows the relative mass change vs. temperature of the Y_2O_3–C mixture in argon–chlorine atmosphere from room temperature to 925 °C. The carbon contents evaluated were 0, 6.7 and 8.7% (the relative mass change ($\Delta m/m_{0Y_2O_3}$) is calculated with the oxide initial mass) and the conditions used were a heating rate of 3.8 °C/min, Q_{Ar-Cl_2} of 2 L/h and pCl_2 of 35 kPa.

The sample without carbon (curve 1) experiences a considerable mass gain at about 650 °C until it reaches 0.24 of relative mass

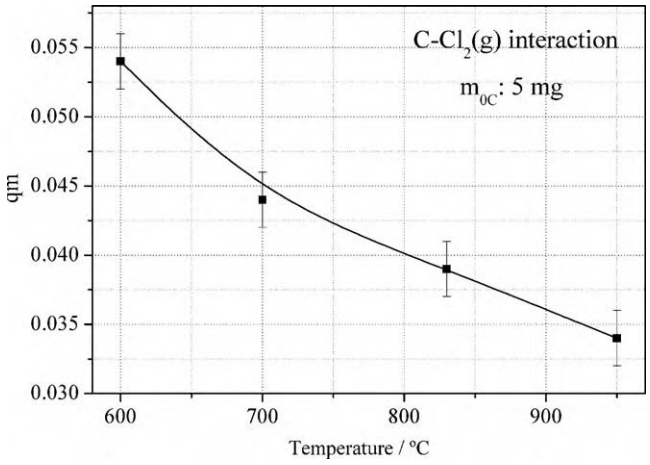

Fig. 5. Maximum relative mass change vs. temperature for the C–Cl_2(g) interaction.

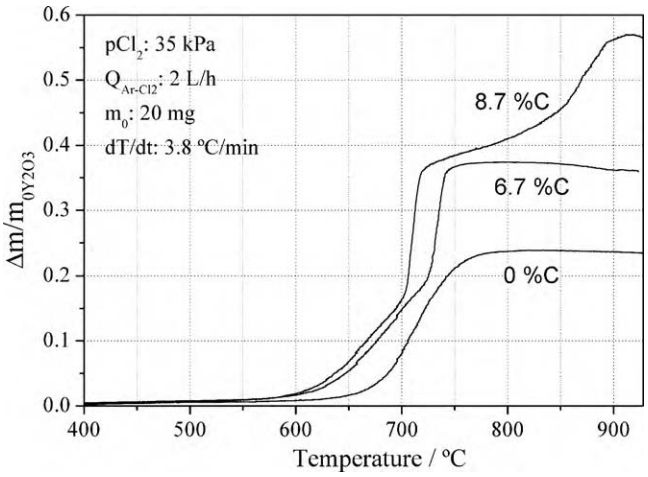

Fig. 6. Non-isothermal thermogravimetries of Y_2O_3–C chlorination with different carbon contents.

change. The XRD analysis of the final product showed only the lines of YOCl [12,26 (card number 12-786)].

The mass change starts in the samples carbochlorinated at a temperature of about 600 °C. The first mass change corresponds to the formation of YOCl and the second mass change, which is observed only in the samples carbochlorinated at $\Delta m/m_{0Y_2O_3} \approx 0.20$, is caused by carbochlorination of the YOCl to produce YCl_3. The reaction of formation of YCl_3 starts at 720 and 702 °C for the samples with 6.7 and 8.7%C, respectively. The XRD analysis of the final products (exposed to atmosphere) in these samples resulted YOCl + $YCl_3{\cdot}6H_2O$ (6.7%C) and $YCl_3{\cdot}6H_2O$ (8.7%C) (Fig. 7). The sample with 6.7%C does not form completely the chloride because the carbon content is in defect respect to the minimum value to form YCl_3 by carbochlorination (7.4%, stoichiometry of reaction (11)). The sample with 8.7%C has an excess of 20% respect to this reaction, therefore the carbon content is enough to form the chloride by carbochlorination.

The sample in the thermobalance cannot be retrieved in an airtight way, and the chloride obtained is hydrated. With the objective of obtaining a XRD pattern of the anhydrous YCl_3, a carbochlorination was made in a reactor which is possible to open in a dry glass box. Fig. 8 shows the XRD patterns obtained, verifying that the product is anhydrous yttrium trichloride.

The yttrium trichloride is a white solid with a melting point between 700 and 721 °C [27–31] and a boiling point of 1427–1510 °C [28–30]. The vapor pressure (P_v) has the following

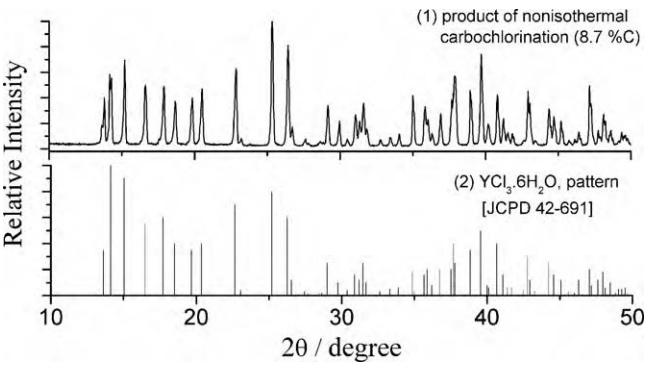

Fig. 7. Diffraction patterns for: (1) product of non-isothermal chlorination of Y_2O_3–C (8.7%C) (exposed to atmosphere); (2) reference pattern of $YCl_3{\cdot}6H_2O$ [26, card number 42-691].

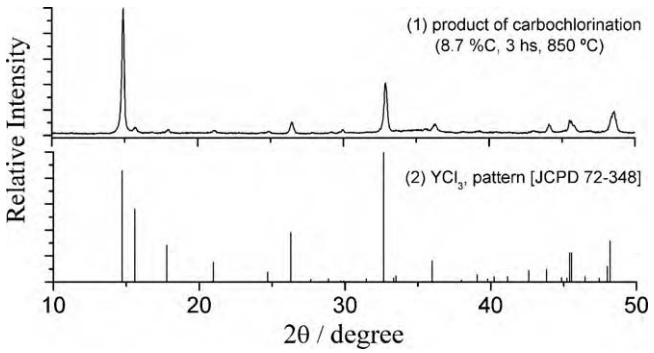

Fig. 8. Diffraction patterns for: (1) product of carbochlorination at 850 °C (the reactor was opened in a dry glass box); (2) reference pattern of YCl_3 [26, card number 72-348].

dependence on the temperature in the range of 700–1000 °C [28]:

$$\ln P_{i\mathrm{YCl_3}} = 18.41 - \frac{249\,\mathrm{kJ/mol}}{R_g \cdot T} \quad \text{(I)}$$

(7×10^{-5} and 2×10^{-3} atm, for 800 and 950 °C, respectively).

However, measurements carried out by us using a DTA/TG analyzer (NETZSCH, STA 409) showed that the melting point of YCl_3 synthesized by chlorination of Y_2O_3–C (8.7%C) is equal to 685 °C. This carbon content was used because the results showed that all carbon is consumed in the reaction, therefore the final product is only YCl_3.

3.4. Reaction stages

Thermogravimetric curves of the non-isothermal carbochlorination of Y_2O_3 showed that the overall reaction consists of several stages (Fig. 6). In order to characterize the reaction products of these stages, carbochlorinations at several temperatures were performed. These experiences were stopped at different conversions and the solid residues were analyzed by XRD. Fig. 9 shows these experiences, which were carried out with the following conditions: 8.7%C, m_0: 10 mg, Q_{Ar-Cl_2}: 4 L/h, pCl_2: 35 kPa.

The text boxes indicate the places where the reactions were stopped and the letter inside represents the phases detected by XRD (a: Y_2O_3 + YOCl; b: YOCl; c: YOCl + YCl_3; d: YCl_3)

The results showed that for temperatures below 600 °C the reaction consists of the carbochlorination of Y_2O_3 to produce YOCl. The reaction at 600 °C in Fig. 9 reaches a value of $\Delta m/m_{0Y_2O_3}$ equal to 0.21 and the characterization of the final product by XRD showed only the diffraction lines of the YOCl. This reaction will be denominated *STAGE I* of the global reaction of carbochlorination of Y_2O_3.

For temperatures above 625 °C the YOCl is carbochlorinated and produces YCl_3, which can be in solid or liquid state. This behaviour is well illustrated in the curve of 850 °C, for which the phases found by XRD were (the values in brackets corresponds to $\Delta m/m_{0Y_2O_3}$): Y_2O_3 + YOCl (0.09); YOCl + YCl_3 (0.42); YCl_3 (0.58). The beginning of this reaction is seen in the thermogravimetric curves as an increase of the reaction rate for $\Delta m/m_{0Y_2O_3}$ lesser than about 0.20 (these value diminishes as temperatures increases).

The diminution in the reaction rate after a value of $\Delta m/m_{0Y_2O_3}$ between 0.33 and 0.37 (the *shoulder* in curves at temperatures above 700 °C) does not involve a change in the products. The characterizations by XRD of the solid residues of the experiences stopped at $\Delta m/m_{0Y_2O_3}$: 0.23 and 0.29 (725 °C), 0.36 (750 °C) and 0.42 (850 °C) showed the presence of YOCl and YCl_3. Therefore, the reaction in the range of $\Delta m/m_{0Y_2O_3}$ of 0.2–0.58 corresponds to the carbochlorination of YOCl to produce YCl_3. The behaviour of the thermogravimetric curve after the shoulder depends on the experimental temperature and its relation with the melting point

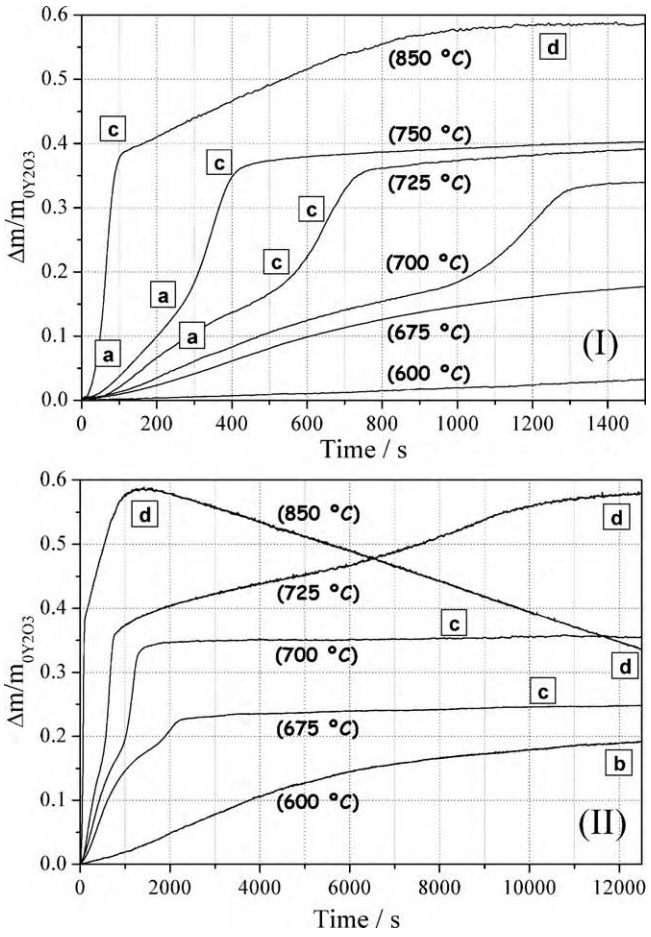

Fig. 9. Isothermal chlorinations of Y_2O_3–C (8.7%C) showing the characterizations by XRD at different values of $\Delta m/m_{0Y_2O_3}$. (I) Until 1500 s; (II) until 12,500 s [XRD characterizations—a: Y_2O_3 + YOCl; b: YOCl; c: YOCl + YCl_3; d: YCl_3].

of YCl_3. For temperatures above 700 °C, after the shoulder the system proceeds with mass gain until it reaches a maximum, where the formation of YCl_3 is complete. For temperatures in the range of 650–700 °C the sample after the shoulder becomes a constant value and the solid residue consists of YOCl + YCl_3.

Then, the reaction of carbochlorination of YOCl to produce YCl_3 will be divided into two successive stages:

STAGE II: *fast* carbochlorination of YOCl, until the shoulder situated at $\Delta m/m_{0Y_2O_3} \approx 0.36$, after which the rate diminishes.
STAGE III: *slow* carbochlorination of YOCl, until the complete formation of YCl_3.

For temperatures higher than 715 °C (8.7%C) the sample mass increases until the complete formation of YCl_3 (the maximum in the thermogravimetric curve) and subsequently the chloride begins to evaporate. In Fig. 9II this evaporation is observed only for the curve at 850 °C, in the curve at 725 °C the mass loss begins for times above the times shown. The evaporation of YCl_3 will be denominated *STAGE IV*.

The results showed that the overall reaction of carbochlorination of Y_2O_3 consists of four successive stages. In Table 1 it is summarized, for the Y_2O_3–C samples with 8.7 and 16.7%C, the reactants and products of each stage (with their state of aggregation), and the ranges of $\Delta m/m_{0Y_2O_3}$ and temperature in which they were observed.

Table 1
Characterization of the stages involved in the chlorination of Y_2O_3–C (0, 8.7, 16.7%C).

STAGE	Reactants	Products	Range of $\Delta m/m_{0Y_2O_3}$	Temperature range (°C)		
				0%C[a]	8.7%C	16.7%C
I	Y_2O_3(s) C(s) Cl_2(g)	YOCl(s) CO(g) CO_2(g) O_2(g)	0–0.23	≥575 °C	≥560 °C	≥550 °C
II	YOCl(s) C(s) Cl_2(g)	YCl_3(l) CO(g) CO_2(g)	0.23–0.38	≥750 °C	≥625 °C	≥575 °C
III	YOCl(s) C(s) Cl_2(g)	YCl_3(l) CO(g) CO_2(g)	0.38–0.65	–	≥715 °C	≥700 °C
IV (YCl_3 evaporation)	YCl_3(l)	YCl_3(g)	Mass loss after the maximum	–	≥715 °C	≥715 °C

[a] In direct chlorination C is not a reactant and instead of CO/CO_2(g) there is only O_2(g) as gaseous product.

3.5. Stoichiometry

The stoichiometry of the reactions of carbochlorination of metallic oxides has not been deeply investigated. Most of the works propose that the reaction proceeds with formation of CO_2 or CO (not both): for temperatures below 800 °C with production of CO_2 and for temperatures above 800 °C with production of CO. These proposals are based on thermodynamic considerations, mainly in the Boudouard reaction (reaction (13)) which regulates the equilibrium between CO_2 and CO in the presence of C.

The stoichiometry was obtained through *mass balances* (taking into account the chlorine adsorbed by the remainder carbon). For comparison, the stoichiometry was also calculated assuming that the system reaches the thermodynamic equilibrium and analyzing the CO_2 and CO amounts. This section will be divided in *STAGE I* ($Y_2O_3 \rightarrow$ YOCl) and *global reaction* ($Y_2O_3 \rightarrow YCl_3$).

3.5.1. Stoichiometry of STAGE I

Fig. 10 shows the results obtained for the *STAGE I* of the *consumed carbon-initial yttrium oxide mass ratio* ($C_{cons}/m_{0Y_2O_3}$). The temperatures analyzed were 600, 625 and 650 °C. Curve (1) represents the value of this relationship when the formation of YOCl progresses with production of CO_2 (reaction (8)) and curve (2) corresponds to the stoichiometry of reaction (9) (formation of CO). All mixtures Y_2O_3–C analyzed have carbon in excess respect to the stoichiometry of reaction (9).

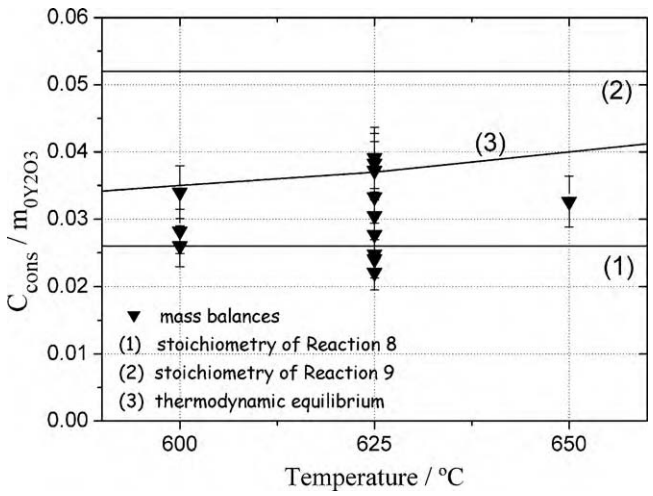

Fig. 10. Relationship between *consumed carbon mass* and *initial Y_2O_3 mass* in carbochlorinations whose XRD analysis of the final product showed only the diffraction lines of YOCl.

Curve (3) represents the behaviour expected if the system reaches the thermodynamic equilibrium. The calculations were performed with the HSC 6.0 Software [20] and the phases considered were as follows:

Gaseous phase: Ar–Cl_2–O_2–CO–CO_2; invariant condensed phases: Y_2O_3–C–YOCl

Table 2 shows the results obtained for the amounts in the equilibrium at 600, 625 and 650 °C. It was considered an excess of chlorine and carbon respect to the initial mass of Y_2O_3. The amount of the O_2 is negligible and the relationships between the equilibrium amounts of CO and CO_2, expressed as pCO^2/pCO_2, are equals to the value of the equilibrium constant of reaction (13) (pCO = *moles of CO/total moles in gaseous phase*).

The values of $C_{cons}/m_{0Y_2O_3}$ for *STAGE I* were calculated assuming that Y_2O_3 is fully consumed by carbochlorination (reactions (8) and (9)) and using the amounts of CO and CO_2 of Table 2 through the following expression:

$$\left.\frac{C_{cons}}{m_{0Y_2O_3}}\right|_{\alpha_{Y_2O_3}=1} = \frac{(n_{CO_2}+n_{CO})\cdot PM_C}{(2\cdot n_{CO_2}+n_{CO})\cdot PM_{Y_2O_3}} = \frac{(n_{CO_2}+n_{CO})\cdot 12}{(2\cdot n_{CO_2}+n_{CO})\cdot 225.812} \quad \text{(II)}$$

where $\alpha_{Y_2O_3}$ is the conversion respect to Y_2O_3, PM_C and $PM_{Y_2O_3}$ are the molecular weights of C and Y_2O_3, respectively and n_{CO_2} and n_{CO} are the mole numbers of the CO_2 and CO in the equilibrium, respectively.

The results obtained from mass balances are indicated with *triangle symbols*. These values were obtained from the calculation of the amount of consumed carbon (C_{cons}) in carbochlorinations that progressed until the complete formation of YOCl (verified by XRD analysis). The procedure consisted of calculating the final mass

Table 2
Equilibrium phase composition in the Y_2O_3–C–Cl_2 system with formation of YOCl (30% excess of chlorine, 16.7%C, pCl_2: 35 kPa, total pressure 101.3 kPa).

Species	Initial amount (mol)	Equilibrium amount		
		600 °C	625 °C	650 °C
Gaseous phase		mol	mol	mol
Ar	2.47	2.47	2.47	2.47
Cl_2	1.3	0.3	0.3	0.3
O_2	–	7.24E−25	2.82E−24	9.72E−24
CO	–	0.321	0.417	0.520
CO_2	–	0.339	0.292	0.240
Invariant condensed phases		mol	mol	mol
Y_2O_3	1	–	–	–
C	3.77	3.11	2.91	2.8
YOCl	–	2	2	2

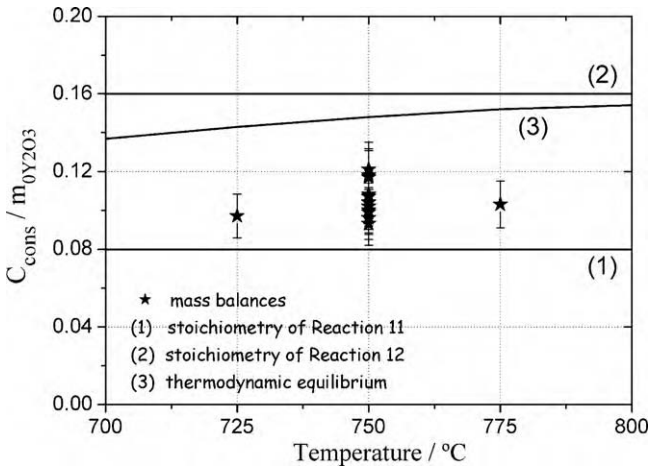

Fig. 11. Relationship between *consumed carbon mass* and *initial Y_2O_3 mass* when Y_2O_3 is fully consumed producing YCl_3 (α_{YOCl}: 1).

present in the crucible from the maximum mass gain observed by thermogravimetry. The final sample is composed by the YOCl capable of being formed with the initial mass of Y_2O_3 and unreacted carbon. This carbon has an amount of adsorbed chlorine and it is necessary to subtract it. This amount was estimated from the results summarized in Fig. 5. The results show that the consumed carbon was never enough such the reaction progresses with the formation of CO (reaction (9)) and the values of $C_{cons}/m_{0Y_2O_3}$ are similar to those obtained assuming the system reaches the thermodynamic equilibrium.

From the average of the mass balance results is possible to calculate a stoichiometry for *STAGE I*, taking into account the following assumptions: (1) the direct chlorination is negligible and the YOCl is produced by carbochlorination. At 600 °C the values of mass change rates are 2.3×10^{-6}, 29×10^{-6} and 36×10^{-6} seg^{-1} for 0, 8.7 and 16.7%C, respectively; (2) the stoichiometry is constant in the temperature range analyzed. Therefore, the stoichiometry can be written as:

$$Y_2O_3(s) + (w/2)C(s) + 3Cl_2(g) \rightarrow 2YOCl(s) + (w-1)CO(g) + (1-w/2)CO_2(g) \quad (19)$$

where w has values between 1 and 2 (1 for only CO_2 and 2 for only CO). The average value of $C_{cons}/m_{0Y_2O_3}$ is equal to 0.031 and the stoichiometry resulting is:

$$Y_2O_3(s) + 0.58C(s) + Cl_2(g) \rightarrow 2YOCl(s) + 0.16CO(g) + 0.42CO_2(g) \quad (20)$$

3.5.2. Stoichiometry of global reaction

In this section is analyzed the stoichiometry of the global reaction of carbochlorination of Y_2O_3 that leads to the formation of YCl_3. Fig. 11 shows the results obtained for the relation $C_{cons}/m_{0Y_2O_3}$. Curve (1) represents the value of this relationship when the formation of YCl_3 progresses with production of CO_2 (reaction (11)) and curve (2) corresponds to the stoichiometry of reaction (12) (formation of CO). All mixtures Y_2O_3–C analyzed have carbon in excess respect to the stoichiometry of reaction (12).

Curve (3) represents the behaviour expected if the system reaches the thermodynamic equilibrium.

The calculations of the equilibrium composition are shown in Table 3 and the relation $C_{cons}/m_{0Y_2O_3}$ is obtained from the following

Table 3
Equilibrium phase composition in the Y_2O_3–C–Cl_2 system with formation of YOCl and YCl_3 (30% excess of chlorine, 16.7%C, pCl_2: 35 kPa, total pressure 101.3 kPa).

Species	Initial amount (mol)	Equilibrium amount		
		725 °C	750 °C	775 °C
Gaseous phase		mol	mol	mol
Ar	7.4	7.4	7.4	7.4
Cl_2	3.9	0.9	0.9	0.9
O_2	–	5.882E−22	1.312E−21	2.711E−21
CO	–	2.389	2.574	2.710
CO_2	–	0.305	0.213	0.145
YCl_3	–	8.967E−5	1.915E−4	3.922E−4
Invariant condensed phases		mol	mol	mol
Y_2O_3	1	–	–	–
C	3.77	1.075	0.983	0.915
YOCl	–	–	–	–
YCl_3		2	2	2

expression:

$$\left.\frac{C_{cons}}{m_{0Y_2O_3}}\right|_{\alpha_{YOCl}=1} = \frac{(n_{CO_2}+n_{CO})\cdot PM_C}{(2/3\cdot n_{CO_2}+1/3\cdot n_{CO})\cdot PM_{Y_2O_3}} = \frac{(n_{CO_2}+n_{CO})\cdot 12}{(2/3\cdot n_{CO_2}+1/3\cdot n_{CO})\cdot 225.812} \quad (III)$$

where α_{YOCl} is the conversion respect to the YOCl produced in *STAGE I*.

Star symbols represent the results obtained through mass balances performed on the maximum of the thermogravimetric curves for carbochlorinations carried out at 725, 750 and 775 °C. At these temperatures the evaporation of the YCl_3 produced is negligible for the time at which the maximum was reached. Therefore, the compounds in the crucible are the YCl_3 produced with the initial mass of Y_2O_3 and unreacted carbon. The carbon has adsorbed chlorine, which was subtracted through the correspondent value of *qm* (Fig. 5). The results show that the consumed carbon is lower than those predicted by thermodynamics, and the stoichiometry of the global reaction calculated from the average $C_{cons}/m_{0Y_2O_3}$ is the following:

$$Y_2O_3(s) + 2C(s) + 3Cl_2(g) \rightarrow 2YCl_3(l) + CO(g) + CO_2(g) \quad (21)$$

3.6. Morphological analysis

Fig. 12 shows the evolution of the morphology of the Y_2O_3 particles in the *STAGE I* analyzed by SEM. In Fig. 12a is shown a particle of unreacted oxide and Fig. 12b corresponds to a particle of a sample carbochlorinated at 850 °C until a value of $\Delta m/m_{0Y_2O_3} = 0.089$. This value of relative mass gain represents a $\alpha_{Y_2O_3}$ in the range of 0.41–0.47 (0.41 if the reaction produces CO_2 and 0.47 if it forms CO). The XRD analysis of this sample showed the presence of remaining Y_2O_3 and the diffraction lines of YOCl. This new phase is observed in the image as crystals growth on the surface; however the YOCl crystals have grown in the overall volume of the sample. If YOCl nucleates only at the outer surface it should be a higher number of YOCl crystals at the surface in order to have the YOCl necessary to give a conversion of about 0.41–0.47. Fig. 12c and d was taken from a sample reacted at 600 °C until the complete formation of YOCl (confirmed by XRD). The EDS analysis of this sample resulted 53%Y–47%Cl, which is very close to the expected values for a sample of pure YOCl.

The SEM images and the *sigmoidal shape* of the thermogravimetric curves in the *STAGE I* (see curve of 600 °C in Fig. 9II) are showing that the formation of YOCl follows a model of *nucleation and growth*. The same model was observed in the production of YOCl by direct chlorination [12].

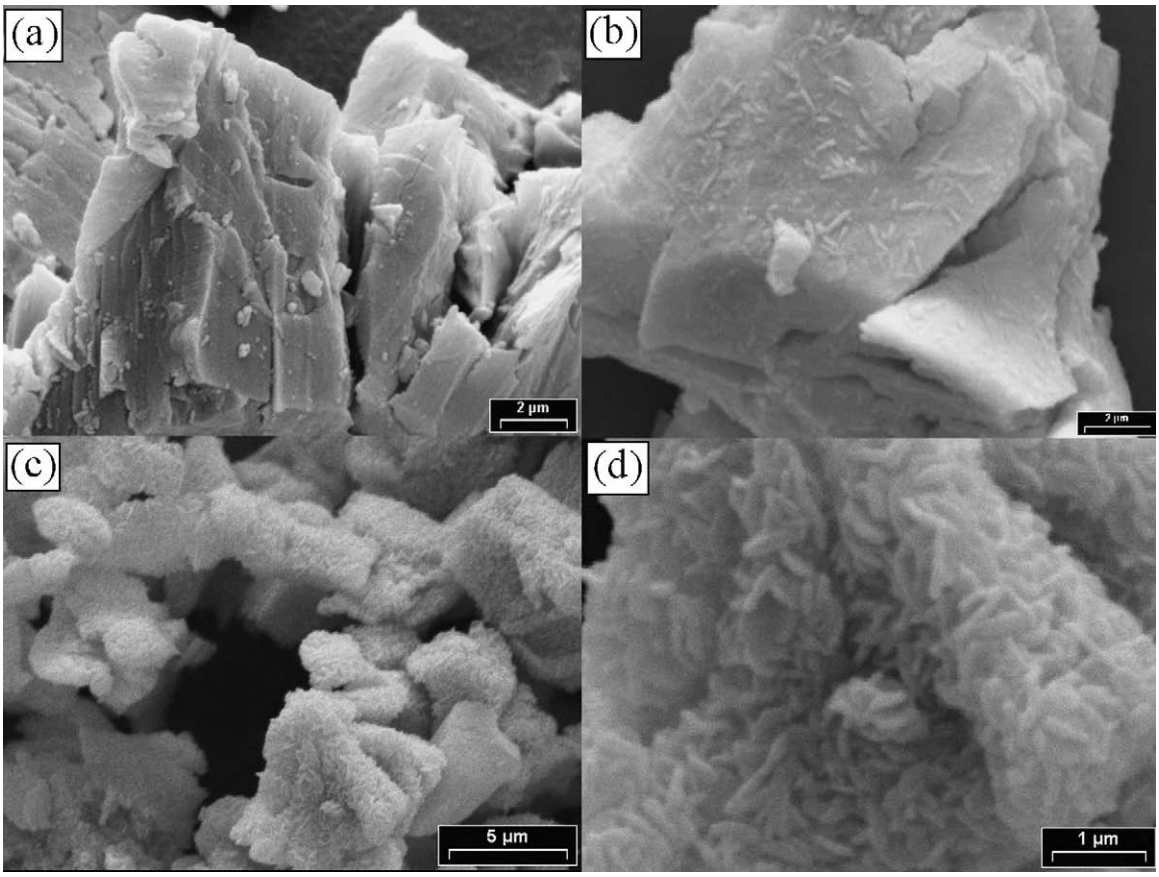

Fig. 12. SEM images of: (a) unreacted Y_2O_3; (b) 850 °C, $\alpha_{Y_2O_3}$: 0.41–0.47; (c) and (d) 600 °C, $\alpha_{Y_2O_3}$: 1.

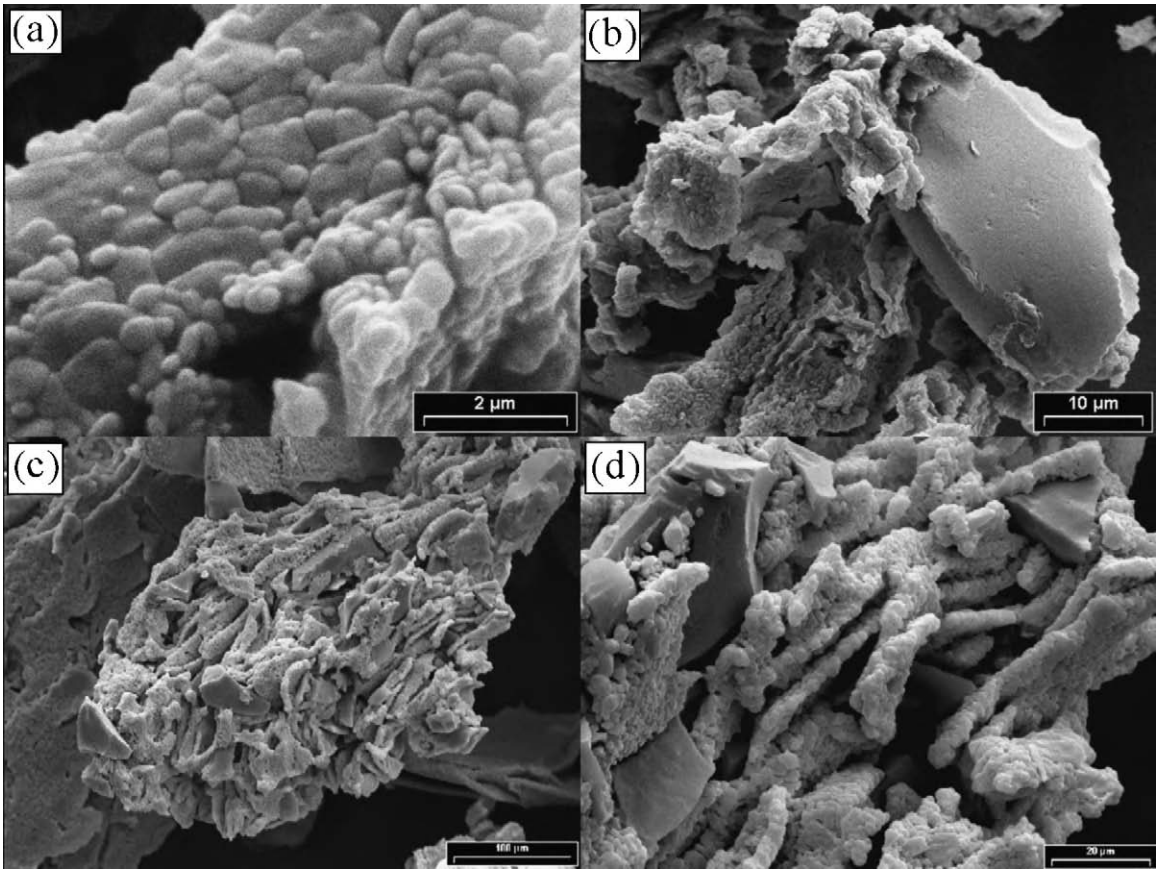

Fig. 13. SEM images of: (a) and (b) 675 °C, α_{YOCl}: 0.08–0.15; (c) 700 °C, α_{YOCl}: 1; (d) 900 °C, α_{YOCl}: 1.

In Fig. 13 is shown the SEM micrographies of samples after the formation of YOCl (*STAGES II and III*). Fig. 13a and b was obtained from samples treated at 675 °C until $\Delta m/m_{0Y_2O_3} = 0.25$ and the XRD analysis of this sample exposed to the atmosphere showed the lines of YOCl and $YCl_3{\cdot}6H_2O$. This value of relative mass gain corresponds to a range of α_{YOCl} equal to 0.08–0.15 (if the global reaction has the stoichiometries of reactions (8) and (15) or (9) and (16), respectively.

Fig. 13c and d shows the images of samples reacted until the complete formation of YCl_3, at 700 and 900 °C, respectively. The XRD analyses of these samples, exposed to the atmosphere, showed only the lines of $YCl_3{\cdot}6H_2O$ and the EDS analysis of a group of crystals of Fig. 13d resulted 25%Y–75%Cl (atomic). The particles with smooth faces correspond to carbon, which are contained inside solidified yttrium chloride. The difference between the morphology of the chloride obtained at 675 and 700 or 900 °C is due to the fact that at 675 °C the chloride is solid, whereas at 700 and 900 °C it is formed in liquid state.

Fig. 14a–c shows the SEM images of the carbon particles at different stages of the reaction. In Fig. 14a is shown an unreacted carbon, which has faces completely smooth. Fig. 14b corresponds to a carbochlorination performed at 600 °C until complete formation of YOCl. The attack on the carbon surface is manifested through the appearance of small holes with little depth. A carbon particle in a higher reaction degree is shown in Fig. 14c which corresponds to a sample reacted at 750 °C up to a value of $\Delta m/m_{0Y_2O_3} = 0.33$ (α_{YOCl} = 0.26–0.37). This image shows one of the ways that the YOCl–C–Cl_2 interaction is performed (the oxide was completely consumed producing YOCl). In this picture, a particle is putted up at a hole inside the carbon particle. This behaviour can be explained taking into account that Cl_2 dissociates on carbon surface [5,32], generating a flow of chlorine atoms ($Cl^{\bullet}$) which produces a strong attack at the YOCl particles. This attack is more favorable as the distance between YOCl and C is shorter, since the chlorine atoms have lower probability of recombination.

3.7. STAGE IV—evaporation of YCl_3

The analysis of the carbochlorination reaction of Y_2O_3 showed that for temperatures above 715 °C and carbon contents higher than 8.7%C the oxide is fully consumed producing YCl_3. Subsequently it is observed in the thermogravimetries a mass loss which corresponds to the evaporation of the chloride (Fig. 9II, curve of 850 °C).

The analysis of the species inside the crucible indicated that there is no remaining carbon after the chlorination of mixtures Y_2O_3–C with 8.7%C. Therefore, at the maximum of the thermogravimetries the sample is composed only by anhydrous YCl_3. The kinetics of the YCl_3 evaporation was studied under Ar atmosphere, for which after the formation of YCl_3 chlorine was diverted from the reaction zone and the flow of argon was adjusted to 4 L/h.

Fig. 15 shows the thermogravimetric curves for the evaporation of YCl_3 synthesized by carbochlorination of Y_2O_3 (8.7%C, m_0: 10 mg) at temperatures between 800 and 950 °C. The curves are straight lines along the whole process; this behaviour is indicating that the evaporation rate does not depend on the YCl_3 mass.

A simple kinetic model for the evaporation of a liquid sample inside the crucible in the thermogravimetric system was developed [33]. This model consider that there is a zone near the sample surface where the YCl_3 molecules are in liquid–vapor pseudoequilibrium and the mass loss detected for the thermobalance is due to the diffusion of the YCl_3 molecules to the gas stream. The expression obtained is the following:

$$\text{Evaporation rate} = \left(\frac{D}{\Delta x}\right) \cdot \left(\frac{P_{vap} \cdot N_A}{R_g \cdot T}\right) \quad \text{(IV)}$$

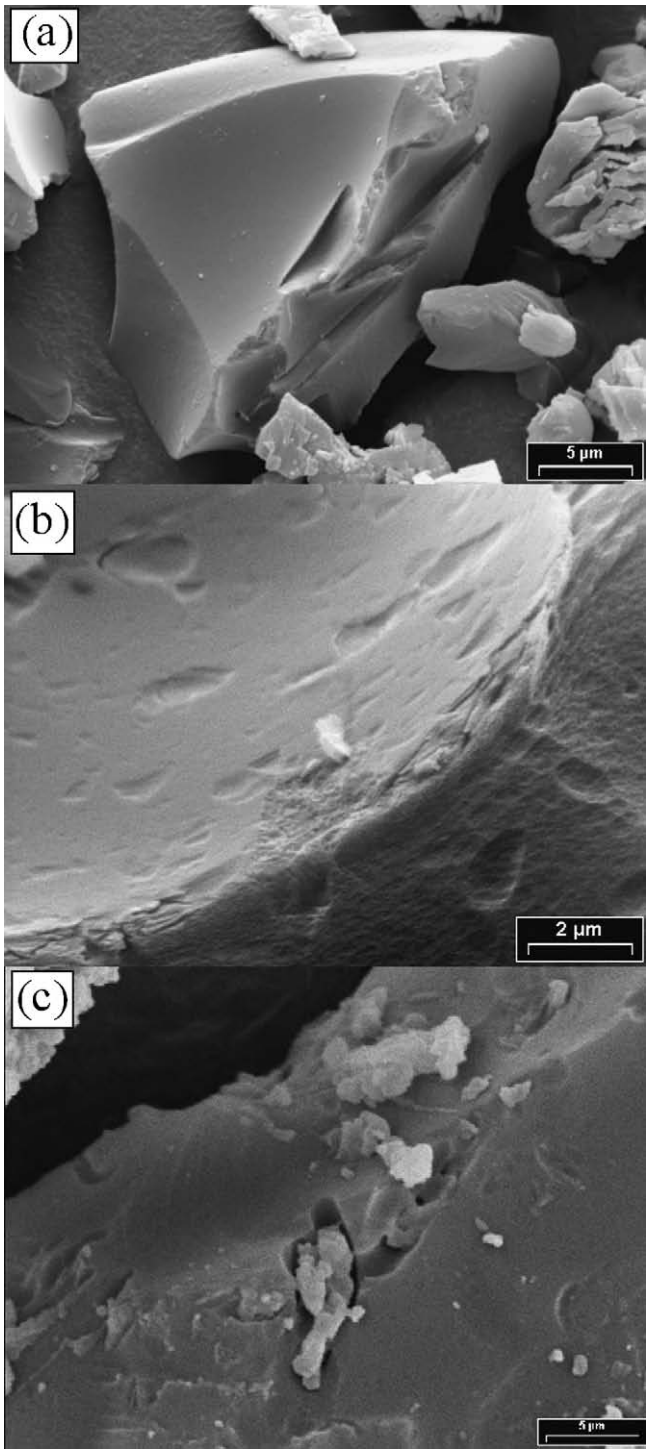

Fig. 14. SEM images of the carbon particles: (a) unreacted carbon; (b) 600 °C, $\alpha_{Y_2O_3}$: 1; (c) 750 °C, α_{YOCl}: 0.26–0.37.

where D is the binary diffusion coefficient YCl_3/Ar, Δx is the layer boundary thickness, P_{vap} is the YCl_3 equilibrium pressure, N_A is the Avogadro number, R_g is the gas constant and T is the temperature.

Replacing P_{vap} by the Clausius–Clapeyron equation [34]:

$$P_{vap} = A' \cdot \exp\left(-\frac{\Delta H_{vap}}{R_g \cdot T}\right) \quad \text{(V)}$$

$$\text{Evaporation rate} = \frac{N_A \cdot A'}{R_g \cdot \Delta x} \cdot \frac{D}{T} \cdot \exp\left(-\frac{\Delta H_{vap}}{R_g \cdot T}\right) \quad \text{(VI)}$$

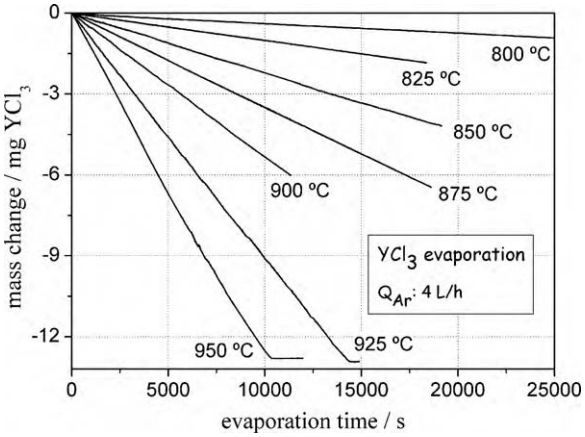

Fig. 15. Effect of the temperature on the evaporation rate of YCl_3 under argon atmosphere.

where A' is a factor independent on the temperature and ΔH_{vap} is the evaporation heat of the YCl_3.

Although D is dependent on the temperature, the factor D/T has a light dependence on the temperature. For example, for Cl_2 diffusing in Ar/Cl_2 mixture, the factor D/T is equal to 1.02×10^{-3} and 1.11×10^{-3} $cm^2 \times s^{-1} \times K^{-1}$ at 800 and 950 °C, respectively (D was calculated from Chapman–Enskog theory [35]). Therefore, can be considered that functionality with temperature is contained in the exponential factor, and applying natural logarithms in Eq. (VI) is obtained the following expression:

$$\ln(\text{evaporation rate}) \cong cte[\neq f(T)] - \frac{\Delta H_{vap}}{R_g} \cdot \frac{1}{T} \quad \text{(VII)}$$

Fig. 16 shows a graphic of ln(evaporation rate) in function of the inverse of the absolute temperature. The values of the evaporation rate were obtained from the curves of Fig. 15. In this figure the rates are in $mg \times s^{-1}$. For converting to molecules $\times s^{-1} \times cm^{-2}$ (the units in Eq. (VII)) is multiplied by N_A, and divided by molecular weight of YCl_3 and evaporation area. These three factors are independent on the temperature and can be considered included in the $cte[\neq f(T)]$.

The data were fitted adequately with a straight line, and from its slope it was obtained a value for ΔH_{vap} equal to 250 ± 17 kJ/mol. This value is in good agreement with those reported in literature: 249 kJ/mol in the temperature range of 700–1000 °C [28] and 249.8 kJ/mol [27]. McKinley [36] performed mass spectrometric measurements of the vapor effusing from a cell containing anhydrous yttrium chloride. He found that there are two important vapor species, YCl_3 and Y_2Cl_6. The evaporation heats of the monomer and dimer were obtained from an Arrhenius plot of the ion-current data. These values were 197 and 310 kJ/mol for YCl_3 and Y_2Cl_6, respectively.

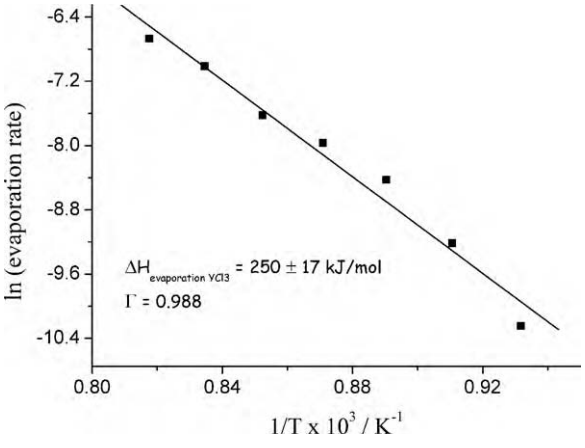

Fig. 16. Plot of Eq. (VII).

The value determined in this work is an intermediate one between those obtained by McKinley. This result can be indicating that in the experimental system used a fraction of the yttrium chloride is evaporated as monomer and other fraction as dimer.

4. Conclusions

Reactive system Y_2O_3–C–Cl_2(g) was analyzed in the range of temperature of 550–950 °C. The results showed that the reaction proceeds through *three successive stages* until the complete formation of YCl_3. The occurrences of these stages depend on the temperature and carbon content and were well characterized for 8.7 and 16.7%C (Table 1). In the *STAGE I* the carbochlorination of Y_2O_3 leads to the formation of YOCl, which is the intermediate product prior to the formation of YCl_3. The stoichiometry of the reaction involved in this stage was calculated from mass balances of the samples carbochlorinated until the complete formation of the oxychloride, obtaining the following result in the temperature range of 600–650 °C:

$$Y_2O_3(s) + 0.58C(s) + Cl_2(g) \rightarrow 2YOCl(s) + 0.16CO(g) + 0.42CO_2(g)$$

The SEM analysis of the partially reacted samples and the typical sigmoidal shape of the thermogravimetric curves showed that this reaction proceeds through a mechanism of *nucleation and growth* of the YOCl phase. *STAGES II* and *III* consist of the carbochlorination of the YOCl with formation of YCl_3. The difference between these stages is the kinetic nature, being called *fast* and *slow* carbochlorination of YOCl. For occurrence of the *STAGE III* the yttrium trichloride must be in liquid state. The stoichiometry of the global reaction of carbochlorination was calculated from mass balances at the maximum of the thermogravimetric curves, in the temperature range of 725–775 °C:

$$Y_2O_3(s) + 2C(s) + 3Cl_2(g) \rightarrow 2YCl_3(l) + CO(g) + CO_2(g)$$

The interaction between the sucrose carbon and chlorine was studied by thermogravimetry, and the effect of temperature and initial mass on the value of the maximum mass gain were analyzed. These results allowed to take into account the chlorine adsorbed on the carbon surface for further use in the mass balances performed to calculate the stoichiometries.

The final product of the carbochlorination for temperatures higher than 700 °C is liquid yttrium trichloride. The melting point measured for this compound is 685 °C and it has a considerable vapor pressure for temperatures above 800 °C. The kinetics of its evaporation was studied under argon atmosphere in the temperature range of 800–950 °C, being formed from a mixture of Y_2O_3–C with 8.7%C such as the final product consist of only YCl_3 because the carbon is consumed completely. A simple kinetic model predicts that an Arrhenius plot of the evaporation rate allows obtaining the evaporation heat of the chloride. A value of 250 kJ/mol was obtained, which is in good agreement with reported data. This value is consistent with a partial dimerization of YCl_3.

Acknowledgements

The authors thank the Agencia Nacional de Promoción Científica y Tecnológica (ANPCyT), Consejo Nacional de Investigaciones Científicas y Técnicas (CONICET), and Universidad Nacional del Comahue for the financial support of this work.

References

[1] W. Kroll, The production of ductile titanium, Trends Electrochem. Soc. 78 (1940) 35–47.
[2] T.H. Okabe, R. Matsuoka, O. Takeda, Recycling Titanium and other Reactive Metal Scraps by Utilizing Chloride Wastes, vol. I, Global Symposium on Recycling Waste Treatment and Clean Technology, España, Madrid, 2004, pp. 893–902, ISBN 84-95520-01-0.
[3] F. Habashi, Handbook of Extractive Metallurgy, Wiley–VCH, 1997, ISBN 3-527-28792-2.
[4] I. Barin, W. Schuler, On the kinetics of the chlorination of titanium dioxide in the presence of solid carbon, Metall. Trans. B 11 (1980) 199–207.
[5] D.M. Pasquevich, J. Andrade Gamboa, A. Caneiro, On the role of carbon in the carbochlorination of refractory oxides, Thermochim. Acta 29 (1992) 209–222.
[6] S.L. Stefanyuk, I.S. Morozov, Kinetics and mechanism of chlorination of minerals (loparite, pyrochlore, zircon and euxenite), Z. Prikl. Khim. 38 (1965) 737–742.
[7] W.E. Dunn Jr., High temperature chlorination of titanium bearing minerals: Part IV, Metall. Trans. B 10 (1979) 271–277.
[8] A. Bergholm, Chlorination of rutile, Trans. Am. Inst. Min. Eng. 221 (1961) 1121–1129.
[9] V.T. Amorebieta, A.J. Colussi, Direct study of the catalytic decomposition of chlorine and chloromethanes over carbon films, J. Phys. Chem. Kinet. 17 (1985) 849–858.
[10] D.M. Pasquevich, PhD Thesis, Facultad de Ciencias Exactas de la Universidad Nacional de La Plata, 1990.
[11] J.F. Miller, S.E. Miller, R.C. Himes, Preparation of anhydrous rare earth chlorides for physicochemical studies, J. Am. Ceram. Soc. 81 (1959) 4449–4451.
[12] J.P. Gaviría, A.E. Bohé, The kinetics of the chlorination of yttrium oxide, Metall. Trans. B 40 (2009) 45–53.
[13] A.I. Braginski, A.O. Isenberg, M.T. Miller, T.R. Oeffinger, Chlorination of yttrium oxide in presence of carbon, Ceram. Bull. 52 (1972), 630–632/636.
[14] M. Gimenes, H. Oliveira, Microstructural studies and carbochlorination kinetics of xenotime ore, Metall. Trans. B 32 (2001) 1007–1013.
[15] E.B. Augusto, H.P. Oliveira, Kinetics of chlorination and microstructural changes of xenotime by carbon tetrachloride, Metall. Trans. B 32 (2001) 783–791.
[16] G. Morteani, The rare earths; their minerals, production and technical use, Eur. J. Miner. 3 (1991) 641–650.
[17] J. Gonzalez, M. del, C. Ruiz, A. Bohe, D.M. Pasquevich, Oxidation of carbons in the presence of chlorine, Carbon 37 (1999) 1979–1988.
[18] D.M. Pasquevich, A.M. Caneiro, A thermogravimetric analyzer for corrosive atmospheres and its applications to the chlorination of ZrO_2-C mixture, Thermochim. Acta 156 (1989) 275–283.
[19] O. Knacke, O. Kubaschewski, K. Hesselman, Thermochemical Properties of Inorganic Substances, second ed., Springer-Verlag, Berlin, 1991.
[20] HSC 6.12, Chemistry for Windows, Outukumpu Research Oy, Pori, Finland, 2006.
[21] Y.B. Patrikeev, G.I. Novikov, V.V. Badovskii, Thermal dissociation of scandium, yttrium and lanthanum oxide chlorides, Russ. J. Phys. Chem. 47 (1973) 284.
[22] F. Habashi, Principles of Extractive Metallurgy, vol. II, Gordon and Breach Science Publisher, New York, 1980, pp. 172–174.
[23] H. Tobias, A. Soffer, A chemisorption of halogen on carbon—I. Stepwise chlorination and exchange of C–CI with C–H bonds, Carbon 23 (1985) 281–289.
[24] H. Tobias, A. Soffer, Chemisorption of halogen on carbon—II. Thermal reversibility of Cl_2, HCl and H_2 chemisorption, Carbon 23 (1985) 291–299.
[25] A. Landsberg, C. Hoatson, F.E. Block, The chlorination kinetics of zirconium dioxide in the presence of carbon and carbon monoxide, Metall. Trans. 3 (1972) 517–523.
[26] Joint Committee for Powder Diffraction Standards, Powder Diffraction File, International Center for Diffraction Data, Swarthmore, PA, 1996.
[27] R.L. Lide (Ed.), CRC Handbook of Chemistry and Physics, CRC Press LLC, 2005.
[28] I. Barin, Thermochemical Data of Pure Substances, VCH Verlags Gesellschaft, Weinheim, 1993.
[29] F.H. Spedding, A.H. Daane, The rare-earth metals, Met. Rev. 5 (1960) 297–348.
[30] W. Brugger, E. Greinacher, A process for direct chlorination of rare earth ores at high temperatures on a production scale, J. Metals 19 (1967) 32–35.
[31] R.J. Meyer (Ed.), Gmelins Handbuch der Anorganischen Chemie. System N°6 (Cl), Verlag Chemie, Berlin, 1937.
[32] N.V. Manukyan, V.H. Martirosyan, Investigation of the chlorination mechanism of metal oxides by chlorine, J. Mater. Process. Technol. 142 (2003) 145–151.
[33] J.P. Gaviría, PhD Thesis, Universidad Nacional de Cuyo, Instituto Balseiro, S.C. de Bariloche, 2009.
[34] I.N. Levine, Physical Chemistry, 4ª ed., McGraw-Hill, Inc., 1978.
[35] J.O. Hirschfelder, C.F. Curtiss, R.B. Bird, Molecular Theory of Gases and Liquids, Wiley, New York, 1956.
[36] J.D. McKinley, Mass spectrum of yttrium chloride vapor, J. Chem. Phys. 42 (6) (1965) 2245–2246.